Environmental Science
Processes & Impacts

RSC Publishing

PAPER

View Article Online
View Journal | View Issue

Cite this: *Environ. Sci.: Processes Impacts*, 2013, **15**, 1752

Composition and structural effects on the adsorption of ionic liquids onto activated carbon

Jesús Lemus,*[a] Catarina M. S. S. Neves,[b] Carlos F. C. Marques,[b] Mara G. Freire,[b] João A. P. Coutinho[b] and Jose Palomar[a]

Received 6th May 2013
Accepted 9th July 2013

DOI: 10.1039/c3em00230f

rsc.li/process-impacts

The applications and variety of ionic liquids (ILs) have increased during the last few years, and their use at a large scale will require their removal/recovery from wastewater streams. Adsorption on activated carbons (ACs) has been recently proposed for this aim and this work presents a systematic analysis of the influence of the IL chemical structures (cation side chain, head group, anion type and the presence of functional groups) on their adsorption onto commercial AC from water solution. Here, the adsorption of 21 new ILs, which include imidazolium-, pyridinium-, pyrrolidinium-, piperidinium-, phosphonium- and ammonium-based cations and different hydrophobic and hydrophilic anions, has been experimentally measured. This contribution allows an expansion of the range of IL compounds studied in previous works, and permits a better understanding of the influence of the IL structures through the adsorption on AC. In addition, the COSMO-RS method was used to analyze the measured adsorption isotherms, allowing the understanding of the role of the cationic and anionic structures in the adsorption process, in terms of the different interactions between the IL compound and AC surface/water solvent. The results of this work provide new insights for the development of adsorption as an effective operation to remove/recover ILs with very different chemical nature from water solution.

Environmental impact

This work clearly contributes to the development and greater depth of an affordable and easy treatment to remove and/or recover ionic liquids (ILs) from aqueous effluents by adsorption on activated carbons (ACs). This work expands the number of ILs studied to 48 (including six cation families and different hydrophobic and hydrophilic anions) for the adsorption onto commercial AC from the aqueous phase and permits a better understanding of the influence of the IL chemical structures on the adsorption process. In addition, the computational approach based on the quantum-chemical COSMO-RS is effectively applied to justify AC adsorption capacities for different natured ILs, in order to understand the further separation process.

Introduction

Ionic liquids (ILs) are one of the most promising and rapidly developing areas of modern chemistry, technology and engineering, focusing on the final objective of industrial applications.[1,2] ILs present exceptional properties such as negligible vapor pressure and non-flammability under ambient conditions, high thermal and chemical stability, a wide liquid range and high solvent capacity.[3–5] However, probably the most important attribute of ILs is the possibility of designing their properties by an adequate selection of the counterions, so that they can be found nowadays in an outstanding variety. Because of the enormous number of cation and anion combinations, ILs possess a wide spectrum of physical and chemical properties (solubility, polarity, viscosity, *etc.*) and they are already recognized by the chemical industry as new target-oriented reaction and separation media.[6,7] However, the application of ILs at an industrial scale may involve an environmental risk resulting from their transport, storage, and release into the environment through wastewaters.[8,9] Therefore, the removal/recovery of ILs from aqueous streams has to be taken into account for a proper use of ILs in industrial processes, since it has been demonstrated that ILs present a wide range of toxicity and biodegradability.[10–12]

Different treatments have been investigated for the removal of ILs from aqueous effluents. Among the most studied destructive techniques the advanced oxidation[13–15] and biological treatments can be included.[16–18] It is important to consider that in the framework of the development of sustainable processes, the ILs recycling after regeneration or recovery must be envisaged.[8] Amongst the available non-destructive technologies, distillation,[19] crystallization,[20] nanofiltration,[21] pervaporation,[22] separation treatment by using salts[23] and adsorption

[a]*Sección de Ingeniería Química (Departamento de Química Física Aplicada), Universidad Autónoma de Madrid, Cantoblanco, 28049 Madrid, Spain. E-mail: jesus.lemus@uam; Tel: +34 914973598*

[b]*Departamento de Química, CICECO, Universidade de Aveiro, 3810-193 Aveiro, Portugal*

onto solids[24–32] are being increasingly studied. Adsorption onto activated carbons (ACs) has been recently demonstrated to be an effective and non-destructive technique for the removal of imidazolium-based ILs from aqueous solutions and their recovery for further use.[26,27,29–32] ACs are interesting candidates among other adsorbents[33] due to their high surface area, surface chemistry tailoring, harmfulness to the environment and easy handling in operation.[34] Previous adsorption equilibrium studies by our group[26,27] confirmed that the structural properties and the chemical surface of the AC can be conveniently modified to adsorb efficiently imidazolium-based ILs with different chemical nature, indicating the viability of IL adsorption from a thermodynamic point of view. Otherwise, the kinetic aspects of adsorption of ILs onto ACs have been recently discussed,[30] showing that the relatively low adsorption rate of the IL can be efficiently enhanced by decreasing the adsorbent particle size.

In the current work, the investigation of ILs adsorption onto AC in aqueous solution is extended by measuring the equilibrium isotherms of 21 new ILs based on 6 different cation families (imidazolium, pyridinium, ammonium, phosphonium, piperidinium and pyrrolidinium), including different lengths of alkyl side chains and 6 different anions. By expanding the range of ILs studied in previous works[26,27] to a total of 48, it was possible to perform an exhaustive study of the influence of their structures on the adsorption of ILs onto AC. The main objective is to analyze the influence of structural IL elements on the adsorption capacity of a commercial AC to recover the IL solute from water solution. For this purpose, experimental measurements were complemented by the quantum-chemical COSMO-RS method, which provides thermodynamic property estimations and intermolecular interaction analysis, allowing the understanding of the equilibrium data of IL distribution between AC and water phases from a molecular point of view.

Materials and methods

Materials

A commercial AC supplied by Merck (AC-MkU) was used as the adsorbent. The ILs used in this study as adsorbates were in the highest purity available. The ILs were used without prior purification. Table 1 provides a list of the ILs used in this study and their source and purity.

Adsorption experiments

The equilibrium technique used to determine the adsorption isotherms of ILs onto commercial AC is detailed in previous works.[26,27] The experiments were conducted in stoppered glass bottles (100 mL) at 35 °C, using 50 mL of an IL solution with concentrations ranging from 100 to 1000 mg L^{-1} (all the ILs present solubilities in water higher than this range at 308 K). Then the AC was added and the solutions were placed in an orbital incubator (Julabo Shake Temp, model SW-22) at 200 rpm, and left for four days. After that time, the samples were removed from the bath and analysed.

Apparent distribution coefficients K_d (L kg^{-1}) were calculated to evaluate the capacity (q_e) of AC for the adsorption of the different ILs at identical equilibrium concentration (C_e), as $K_d = q_e/C_e$.

The concentration of imidazolium and pyridinium-based ILs was determined by UV spectroscopy (Varian, model Cary 1E) at 212 nm for the imidazolium ring, 266 nm for the pyridinium ring and 222 nm for the tosylate ring, while the concentration of ammonium, phosphonium-, pyrrolidinium- and piperidinium-based ILs were determined by conductivity measurements (with an uncertainty of ±0.02), at room temperature, using a Mettler Toledo S47 SevenMulti™ dual meter pH/conductivity equipment.[35]

Table 1 Name, acronym, supplier and purity of the ILs used in this work

Name	Acronym	Supplier	Purity
1-Methyl-1-propylpiperidinium bis(trifluoromethylsulfonyl)imide	$[C_3C_1pip][NTf_2]$	Iolitec	99%
3-Methyl-1-propylpyridinium bis(trifluoromethylsulfonyl)imide	$[C_3C_1py][NTf_2]$	Iolitec	99%
1-Methyl-1-propylpyrrolidinium bis(trifluoromethylsulfonyl)imide	$[C_3C_1pyr][NTf_2]$	Iolitec	99%
1-Ethylimidazolium bis(trifluoromethylsulfonyl)imide	$[C_2im][NTf_2]$	Iolitec	98%
1,3-Dimethylimidazolium bis(trifluoromethylsulfonyl)imide	$[C_1C_1im][NTf_2]$	Iolitec	99%
1,3-Diethylimidazolium bis(trifluoromethylsulfonyl)imide	$[C_2C_2im][NTf_2]$	Iolitec	99%
1,3-Dipropylimidazolium bis(trifluoromethylsulfonyl)imide	$[C_3C_3im][NTf_2]$	Iolitec	98%
1-Ethyl-3-propylimidazolium bis(trifluoromethylsulfonyl)imide	$[C_2C_3im][NTf_2]$	Iolitec	99%
1-Ethyl-3-methylimidazolium bis(trifluoromethylsulfonyl)imide	$[C_2C_1im][NTf_2]$	Iolitec	99%
1-Methyl-3-propylimidazolium bis(trifluoromethylsulfonyl)imide	$[C_3C_1im][NTf_2]$	Iolitec	99%
1-Butyl-3-methylimidazolium bis(trifluoromethylsulfonyl)imide	$[C_4C_1im][NTf_2]$	Iolitec	99%
1-Methyl-3-pentylimidazolium bis(trifluoromethylsulfonyl)imide	$[C_5C_1im][NTf_2]$	Iolitec	99%
Tetrabutylammonium chloride	$[N_{4444}]Cl$	Sigma-Aldrich	97%
Tetrabutylphosphonium chloride	$[P_{4444}]Cl$	Cytec	97%
1-Butyl-3-methylimidazolium tosylate	$[C_4C_1im][TOS]$	Iolitec	98%
Tri(isobutyl)methylphosphonium tosylate	$[P_{i(444)1}][TOS]$	Cytec	98%
1-Butyl-3-methylimidazolium methylsulfate	$[C_4C_1im][MeSO_4]$	Iolitec	95%
1-Butyl-3-methylimidazolium octylsulfate	$[C_4C_1im][OcSO_4]$	Iolitec	95%
1-Butyl-3-methylimidazolium acetate	$[C_4C_1im][MeCOO]$	Sigma-Aldrich	95%
1-Ethylpyridinium hexafluorophosphate	$[C_2py][PF_6]$	Iolitec	99%
1-Hexylpyridinium hexafluorophosphate	$[C_6py][PF_6]$	Iolitec	99%

Computational details

The molecular geometry of all molecular models (AC, water and ILs) were optimized at the B3LYP/6-31++G** computational level in the ideal gas-phase using the quantum chemical Gaussian03 package.[36] Vibrational frequency calculations were performed for each case to confirm the presence of an energy minimum. Then, the standard procedure was applied for COSMO-RS calculations, which consists of two steps: first, Gaussian03 was used to compute the COSMO files. The ideal screening charges on the molecular surface for each species were calculated by the continuum solvation COSMO model using the BVP86/TZVP/DGA1 level of theory.[37,38] Subsequently, COSMO files were used as an input in the COSMOtherm[39] code to calculate the thermodynamic properties of the binary IL–AC/H_2O mixtures [interaction energy between IL and AC (E_{IL-AC}) or H_2O (E_{IL-H2O})] and the ternary systems involved in the adsorption phenomena [partition coefficient of IL between water and AC phases (log P)]. The computational approach is detailed elsewhere[26,27] and describes IL adsorption by an ion-pair structure, the aqueous media by an individual water molecule and the AC adsorbent by a mixture of two AC structures, in order to introduce in the simulation the measured concentration of oxygenated groups of the AC-MkU activated carbon.[26] The AC/water partition coefficient (log P) of IL at infinite dilution was calculated by COSMO-RS at 298 K. According to our chosen quantum method, the functional and the basis set, we used the corresponding parameterization (BP_TZVP_C30_0210) for COSMO-RS calculations in the COSMOtherm code.

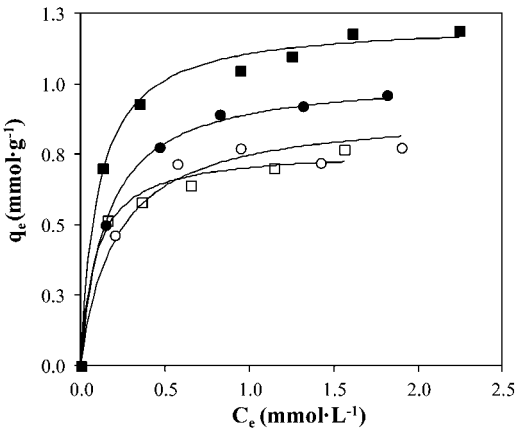

Fig. 1 Experimental equilibrium data (dots) and Langmuir fits (curves) for the adsorption isotherms onto AC-MkU at 308 K of (□), [C_3C_1pip][NTf_2]; (○), [C_3C_1pyr][NTf_2]; (●), [C_3C_1im][NTf_2] and (■), [C_3C_1py][NTf_2].

Results and discussion

The adsorption from water solution of 48 ILs onto a commercial AC supplied by Merck (AC-MkU), which presents a surface BET area of 927 m^2 g^{-1} with high micropore volume contribution ($V_{microp.}$ = 0.36 cm^3 g^{-1} and $V_{mesop.}$ = 0.14 cm^3 g^{-1}) and a relatively low concentration of surface functional groups,[40] was measured. This AC-MkU was previously reported as an effective adsorbent to remove imidazolium ILs from aqueous solution, being its adsorption capacity strongly determined by the hydrophobic/hydrophilic character of the anion and the cation constituting the IL, as a consequence of the different interactions such as polar, van der Waals and hydrogen bonding.[26,27] The wide range of ILs investigated in the current study allows a systematic evaluation of the influence of the cation family, anionic and cationic substituents and the type of anion on the adsorption of the IL onto AC-MkU.

Fig. 1 shows the adsorption isotherms at 308 K of four ILs with a common anion ($[NTf_2]^-$) and alkyl side chain (C_3C_1) and different head groups, as representative cases of pyridinium, imidazolium, pyrrolidinium and piperidinium families. The results indicate that ILs with the cation based on the aromatic ring present higher adsorption capacity than the corresponding aliphatic ones, following the order pyridinium > imidazolium > pyrrolidinium > piperidinium.

Another factor to be taken into account is the number and size of the alkyl chain substituents on the cation. The adsorption isotherms presented in Fig. 2 allow the evaluation of the effect of these structural differences on the adsorption for a series of [$C_nC_n$im][NTf_2] with different chain lengths. The results show that the increase of the number of carbon atoms in the alkyl chain of the imidazolium cation increases the adsorption with a maximum value for [C_5C_1im][NTf_2], for the cases studied. The adsorption seems to be proportional to

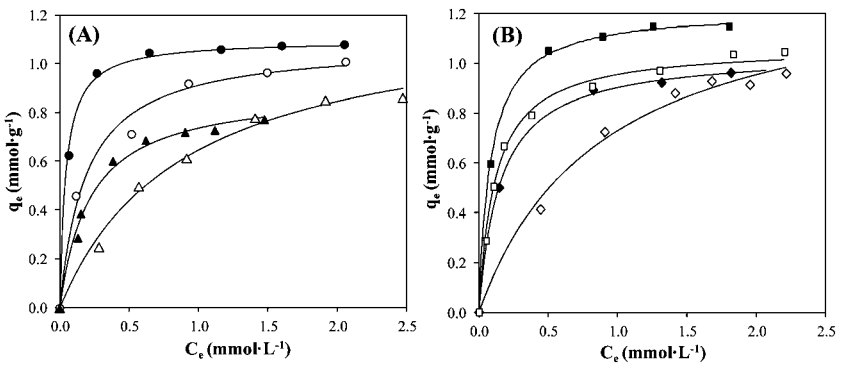

Fig. 2 Experimental equilibrium data (dots) and Langmuir fits (curves) for the adsorption isotherms onto AC-MKU at 308 K of [NTf_2]-based ILs combined with the cation: (A), (△), [C_1C_1im]$^+$; (▲), [C_2C_2im]$^+$; (○), [C_2C_3im]$^+$; (●), [C_3C_3im]$^+$; (B), (◇), [C_2im]$^+$; (◆), [C_3C_1im]$^+$; (□), [C_4C_1im]$^+$ and (■), [C_5C_1im]$^+$.

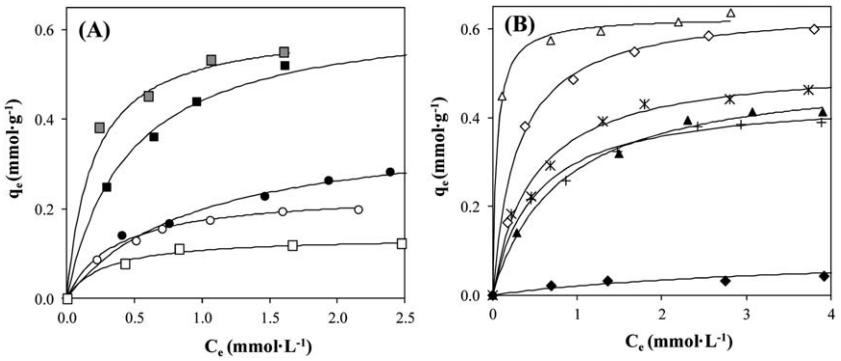

Fig. 3 Experimental equilibrium data (dots) and Langmuir fits (curves) for the adsorption isotherms onto AC-MkU at 308 K of (A) (■), [C_4C_1im][TOS]; (■), [C_4C_1im]-[OTf];[26] (●), [C_4C_1im][TFA] (1-butyl-3-methylimidazolium trifluoroacetate);[26] (○), [C_4C_1im][MeCOO]; (□), [C_4C_1im][$MeSO_3$];[26] (B) (△), [C_4C_1im][$OcSO_4$]; (◇), [C_8C_1im]-Cl;[26] (*), [BzC_1im]Cl;[26] (▲), [C_4C_1im][$MeSO_4$]; (+), [C_6C_1im]Cl and (◆), [C_2C_1im]Cl.[27]

the molar volume of the cation, relating the total number of carbon atoms in its substituents that presents similar adsorption on AC-MkU ($C_1C_1 \sim C_2$, $C_1C_3 \sim C_2C_2$, $C_4C_1 \sim C_2C_3$ and $C_5C_1 \sim C_3C_3$), with the asymmetric cations being slightly more adsorbed onto AC-MkU.

The functionalization of the anion was investigated in order to establish what characteristics produce ILs with a higher affinity towards the AC. Fig. 3A shows the measured adsorption isotherms at 308 K for five [C_4C_1im][X] ILs. Regarding the sulfonate-based anions [R–SO_3], it is possible to observe that the benzyl substituent ([TOS]$^-$) promotes the highest uptake, followed by the CF_3–([OTf]$^-$, triflate) and the CH_3–([$MeSO_3$]$^-$, methylsulfonate). Similar substituent effects are observed for acetate-based ([R–COO]) anions (Fig. 3A), but with a much less remarkable effect. Fig. 3B shows that an increment in the number of carbon atoms in the alkyl chain of the anion (for example, from methylsulfate to octylsulfate) enhances remarkably the adsorption capacity in a similar way to that of increasing the length of the alkyl chain of the imidazolium cation with a common anion (such as from [C_2C_1im]Cl to [C_8C_1im]Cl). Moreover, it is found that the presence of aromatic substituents in the cation (as in [BzC_1im]Cl) also leads to higher adsorption capacities onto AC-MkU (Fig. 3B), with a similar effect to that observed when this substituent is present in the anion.

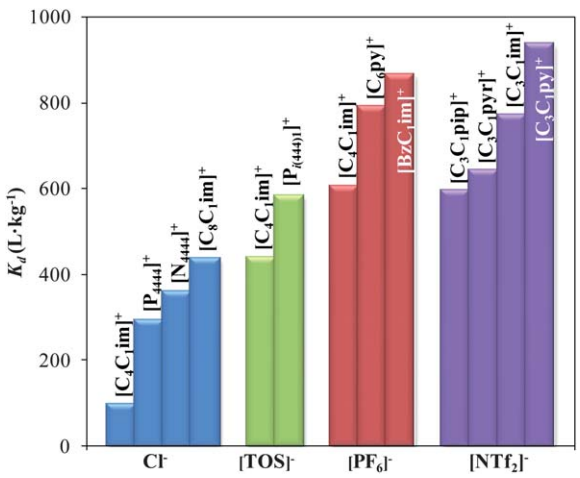

Fig. 4 Comparison of K_d (obtained when $C_e = 1.2$ mmol L^{-1} on AC-MkU at 308 K) for different ionic liquids.

Finally, Fig. 4 shows a summary of the effects of the anion on IL adsorption for various cation families in terms of the apparent adsorption coefficient (K_d) obtained from the experimental isotherms at 308 K with AC-MkU. It can be appreciated that ILs based on the hydrophobic anion such as [NTf_2]$^-$ and [PF_6]$^-$ present the highest adsorption, independent of the cation, which indicates a major influence of the nature of the anion on the adsorption of ILs by ACs from aqueous solution. However, the type of cation also clearly affects the amount of IL adsorbed by AC-MkU, where a more efficient adsorption is achieved when the hydrophobic or the aromatic character of the cation is increased.

In order to better understand the adsorption behaviour of the ILs from aqueous solutions onto ACs, an analysis based on the COSMO-RS method was carried out. Table 2 reports the COSMO-RS predicted values of molecular volume (Å^3) of the ILs and partition coefficients (log P) of IL between AC and H_2O phases at infinite dilution and the experimentally obtained apparent adsorption coefficient (K_d) values onto the AC-MkU at 308 K for the 48 ILs studied so far,[26,27] arranged by experimental adsorption capacity. Fig. 5 compares the experimental K_d and the theoretical log P values for 33 imidazolium-based ILs with a molecular volume below 0.4 nm^3, since it is reported that ILs with higher molecular size present lower adsorption onto AC due to steric effects.[27] The results show a good correlation between experimental and theoretical values for a wide array of 33 IL compounds, indicating the suitability of the COSMO-RS approach to describe the adsorption behaviour of ILs onto ACs from aqueous solution.

Besides the partition coefficient, the COSMO-RS allows the discrimination between the contribution of polar-Misfit, H-bonding and van der Waals forces to the interaction energy between the IL and AC (E_{IL-AC}) and H_2O (E_{IL-H2O}) components involved in the adsorption process. Fig. 6–10 describe the influence of the IL structural components on the interaction energy of the IL solute with the pure AC (E_{IL-AC}) and H_2O

Table 2 Supplier, molecular volume, log *P* of IL calculated by COSMO-RS and experimental K_d (obtained for the $C_e = 1.2$ mmol L^{-1} at 308 K using AC-MkU as adsorbent) of checked ILs

Ionic liquid					
Cation	Anion	Supplier	Molecular Volume (Å^3)	log *P*	K_d (L kg^{-1})
$[C_8C_1im]$	$[PF_6]$	Iolitec	389	3.860	*1008*
$[C_5C_1im]$	$[NTf_2]$	Iolitec	439	4.418	*945*
$[C_3C_1py]$	$[NTf_2]$	Iolitec	406	2.343	936
$[C_3C_3im]$	$[NTf_2]$	Iolitec	434	4.191	883
$[C_{10}C_1im]$	$[PF_6]$	Iolitec	432	4.601	*869*
$[BzC_1im]$	$[PF_6]$	Fluka	354	3.523	*864*
$[C_{10}C_1im]$	$[BF_4]$	Iolitec	402	3.036	*859*
$[C_6C_1im]$	$[PF_6]$	Iolitec	346	2.832	*858*
$[C_{12}C_1im]$	Cl	Iolitec	408	3.914	*825*
$[C_4C_1im]$	$[NTf_2]$	Iolitec	420	4.002	*810*
$[C_6C_1im]$	$[NTf_2]$	Iolitec	463	4.740	*801*
$[C_6py]$	$[PF_6]$	Iolitec	339	2.418	790
$[C_4C_1C_1im]$	$[PF_6]$	Fluka	335	−0.150	*781*
$[C_2C_3im]$	$[NTf_2]$	Iolitec	412	3.947	778
$[C_{14}C_1im]$	Cl	Iolitec	451	4.784	*775*
$[C_8C_1im]$	$[BF_4]$	Iolitec	359	2.112	*772*
$[C_3C_1im]$	$[NTf_2]$	Iolitec	398	3.559	*770*
$[C_{16}C_1im]$	Cl	Iolitec	494	4.729	*733*
$[C_{12}C_1im]$	$[BF_4]$	Iolitec	445	3.965	*729*
$[C_2im]$	$[NTf_2]$	Iolitec	349	3.641	722
$[C_{10}C_1im]$	Cl	Iolitec	365	2.027	*655*
$[C_2C_2im]$	$[NTf_2]$	Iolitec	395	3.473	652
$[C_3C_1pyr]$	$[NTf_2]$	Iolitec	408	2.900	641
$[C_2C_1im]$	$[NTf_2]$	Iolitec	376	3.175	*633*
$[C_4C_1im]$	$[PF_6]$	Iolitec	303	2.061	*605*
$[C_3C_1pip]$	$[NTf_2]$	Iolitec	427	2.763	593
$[C_1C_1im]$	$[NTf_2]$	Iolitec	352	2.915	587
$[P_{i(4441)}]$	[TOS]	Cytec	518	3.723	582
$[C_2C_1im]$	$[PF_6]$	Iolitec	259	1.273	*528*
$[BzC_1im]$	$[BF_4]$	Fluka	298	1.131	*515*
$[C_4C_1im]$	$[OcSO_4]$	Iolitec	451	3.089	503
$[C_6C_1im]$	$[BF_4]$	Iolitec	316	1.172	*465*
$[C_4C_1im]$	[TOS]	Iolitec	363	1.561	439
$[C_8C_1im]$	Cl	Iolitec	322	1.490	*435*
$[N_{4444}]$	Cl	Iolitec	420	3.178	358
$[BzC_1im]$	Cl	Fluka	265	−0.423	*313*
$[P_{4444}]$	Cl	Cytec	425	4.116	292
$[C_2py]$	$[PF_6]$	Iolitec	251	0.889	278
$[C_6C_1im]$	Cl	Iolitec	279	0.585	*264*
$[C_4C_1im]$	[OTf]	Fluka	317	1.496	*258*
$[C_4C_1im]$	$[MeSO_4]$	Iolitec	300	0.048	254
$[C_4C_1im]$	$[BF_4]$	Iolitec	273	0.289	*240*
$[C_4C_1im]$	[TFA]	Fluka	310	2.275	*180*
$[C_4C_1im]$	[MeCOO]	Sigma-Aldrich	268	2.108	127
$[C_4C_1im]$	Cl	Iolitec	236	−0.420	*96*
$[C_2C_1im]$	$[BF_4]$	Iolitec	229	−0.389	*74*
$[C_4C_1im]$	$[MeSO_3]$	Sigma-Aldrich	289	−0.158	*58*
$[C_2C_1im]$	Cl	Iolitec	192	−1.242	*20*

(E_{IL-H2O}) species predicted by COSMO-RS, which is related to the corresponding experimental values of K_d, the adsorption capacity parameter for each IL studied.

Fig. 6 shows the results obtained for a series of anions with a common $[C_4C_1im]$ cation. It can be observed that attractive van der Waals forces dominate the interaction between the IL adsorbate and the AC adsorbent, with higher adsorption capacities of AC-MkU, quantified in terms of experimental K_d,

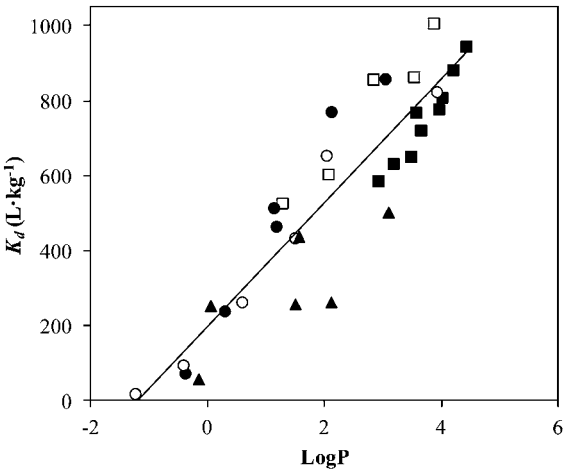

Fig. 5 Experimental K_d *versus* predicted log *P* by COSMO-RS for 32 ILs with a molecular volume below 0.4 nm^3 using AC-MkU as an adsorbent at 308 K: (■), $[NTf_2]^-$; (□), $[PF_6]^-$; (●), $[BF_4]^-$ and (▲), others.

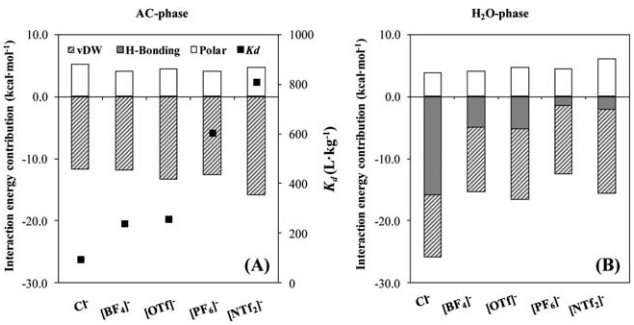

Fig. 6 Predicted COSMO-RS contributions to interaction energies of (A) IL–AC and (B) IL–water for $[C_4C_1im]^+$ based ILs with Cl^-, $[BF_4]^-$, $[PF_6]^-$ and $[NTf_2]^-$ anions.

for more hydrophobic anion-based ILs. This is in good agreement with the increasing attractive van der Waals interactions between IL and the AC surface, described by COSMO-RS. This result is consistent with the enhanced adsorption capacity of hydrophilic IL achieved with chemically treated ACs, which presented higher concentration of oxygenated groups in the adsorbent surface.[27] Therefore, the variation in the anion with

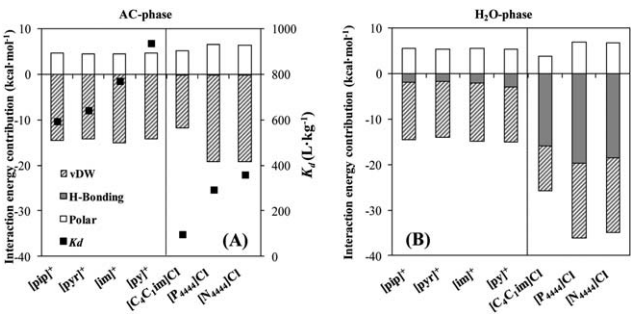

Fig. 7 Predicted COSMO-RS contributions to interaction energies of (A) IL–AC and (B) IL–water for $[NTf_2]^-$ and Cl-based ILs with different cation families.

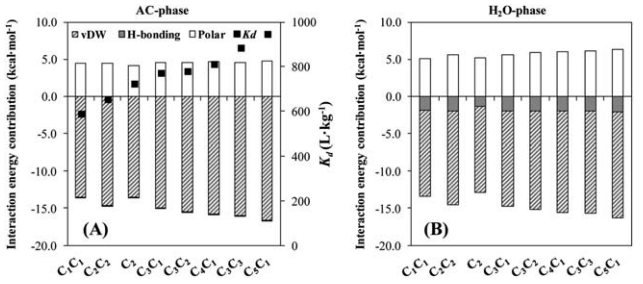

Fig. 8 Predicted COSMO-RS contributions to interaction energies of IL–AC (A) and IL–water (B) for $[C_nC_m\text{im}][NTf_2]$ based ILs with different alkyl chain substituents.

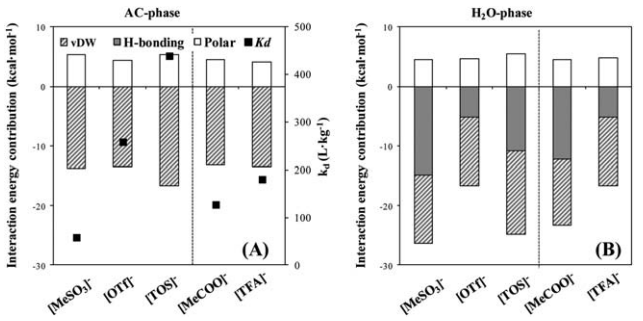

Fig. 9 Predicted COSMO-RS contributions to interaction energies of (A) IL–AC and (B) IL–water for $[C_4C_1\text{im}]^+$ based ILs with different anions.

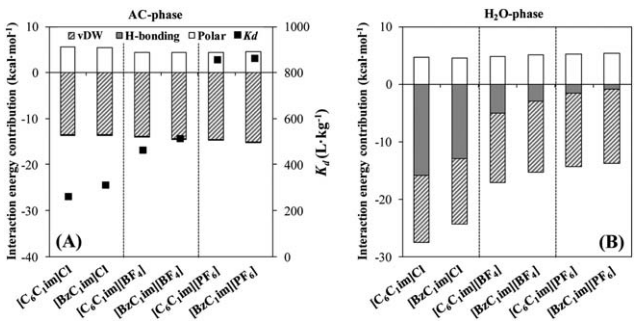

Fig. 10 Predicted COSMO-RS contributions to interaction energies of (A) IL–AC and (B) IL–water for $[C_6C_1\text{im}]^+$ or $[BzC_1\text{im}]^+$ based ILs with Cl^-, $[BF_4]^-$ or $[PF_6]^-$ anions.

remarkably different polarities is translated into different uptakes, where ILs with hydrophobic anions ($[NTf_2]^-$ or $[PF_6]^-$) show much higher adsorption by AC-MkU than hydrophilic ones (Cl^- or $[BF_4]^-$, tetrafluoroborate), due to the stronger attractive van der Waals forces between IL and AC, and the absence of hydrogen bonding interactions between IL and H_2O.

The results of the COSMO-RS analysis of the cation family effect using the series of ILs with a common hydrophobic ($[NTf_2]^-$) or hydrophilic (Cl^-) anion are reported in Fig. 7. It can be concluded again that the favourable van der Waals interactions between ILs and AC control the adsorption of the ILs to the AC-MkU. On the other hand, as it was explained above, favourable hydrogen bonding between chloride-based ILs and water molecules lead to lower K_d values than in the case of $[NTf_2]^-$-based ILs. For the latter, aromatic cations (imidazolium and pyridinium) present higher uptake than cations with aliphatic rings (piperidinium and pyrrolidinium). The COSMO-RS analysis does not provide an explanation for this effect, since similarly IL–AC van der Waals interactions were predicted for all the cations. On the other hand, a better removal of the chloride-based ILs from water is clearly achieved by adsorption when increasing the hydrophobic nature of the cation, from nitrogen heterocyclic-based cations to ammonium and phosphonium tetraalkyl-substituted cations. COSMO-RS analysis indicates that this effect should be assigned to the favourable cation–AC van der Waals interaction rather than hydrogen bonding anion–water interactions.

The effects of the substituents in the cation and the anion of IL on adsorption effectiveness were also considered in the COSMO-RS analysis. Fig. 8 shows that for the imidazolium cation series, based on a common $[NTf_2]^-$ anion, increasing the number of carbon atoms in the alkyl chain induces higher attractive interaction energies between the IL and the AC surface, that is consistent with the higher IL adsorption measured. Similarly, Fig. 9 shows that modifying the substituent of the anion for the case of ILs with sulfonate- and acetate-based anions also leads to changes in the interactions between IL, AC and H_2O components involved in the adsorption process, with the attractive van der Waals interactions increasing in the order $C_6H_5^- > CF_3^- > CH_3^-$, consistently with the adsorption trends described by the K_d values. On the other hand, the significant hydrogen bonding between sulfonate- and acetate-based ILs and water molecules also determines the adsorption thermodynamics, leading to low K_d values, close to those of hydrophilic chloride-based ILs. The addition of an aromatic substituent (as benzyl) to the cation also enhances the adsorption of IL onto AC-MkU as shown in Fig. 10. It seems that the substituents in the cationic or anionic structures of ILs also drive the adsorption uptake. Higher uptakes are achieved for ILs with the benzyl substituent than with a C_6 aliphatic alkyl chain; or with ILs based on anions substituted with $[OTf]^-$ than those substituted with $[MeSO_3]^-$ groups.

In summary, the experimental and theoretical results of this work allowed a detailed analysis of the effect of the structural elements of the IL on the adsorption, such as nature of the cation, cation and anion substituents and nature of the anion, providing new insights into the development of the ILs adsorption on AC from aqueous phases.

Conclusions

This work is focused on the study of the influence of the chemical structures of ILs through their adsorption from water on a commercial activated carbon AC-MkU. Equilibrium adsorption measurements for 21 ILs were carried out with the aim of extending the number of compounds studied previously to a wide range of 48 ILs, which include a variety of anions (11) and cations (20), from imidazolium, pyridinium, ammonium, phosphonium, piperidinium and pyrrolidinium families. It permitted to analyse the effect of the different structural

elements of an IL, such as the head group cation and anion substituents and nature, on the adsorption process. To complement this study, a COSMO-RS analysis was performed to infer on the interaction energies between IL and AC/H_2O components involved in the adsorption process.

The results showed that the IL family has a remarkable influence on the adsorption of ILs on AC: higher uptakes are obtained in the order ammonium > phosphonium > pyridinium > imidazolium > pyrrolidinium > piperidinium promoted by attractive van der Waals interactions between the IL and AC surface. On the other hand, it was also concluded that the substituents of the cation or the anion can also lead to different adsorptions onto AC. Increasing the number of the carbon atoms in the alkyl chains, linked to the cation or the anion, results in higher adsorption coefficients of IL between AC and H_2O phases, due to enhanced IL–AC interactions. Other substituents in the cationic or anionic structures of ILs also lead to different uptake. Thus, higher uptakes are found for ILs with benzyl substituents than the corresponding ILs with a linear alkyl chain; or with ILs based on anions substituted with CF_3– than those substituted with CH_3– groups. Finally, the variation on the anion with remarkably different polarities is translated into different results, where ILs with hydrophobic anions ($[NTf_2]^-$ or $[PF_6]^-$) show much higher adsorption onto AC-MkU than more hydrophilic ILs (Cl^- or $[BF_4]^-$), due to the stronger attractive van der Waals interactions between IL and AC, and the absence of hydrogen bonding interactions between IL and H_2O.

Acknowledgements

The authors are grateful to the Spanish "Ministerio de Ciencia e Innovación (MICINN)" and "Comunidad de Madrid" for financial support (projects CTQ2011-26758 and S2009/PPQ-1545). We are very grateful to "Centro de Computación Científica de la Universidad Autónoma de Madrid" for computational facilities. The authors also acknowledge FCT – *Fundação para a Ciência e a Tecnologia*, through the projects Pest-C/CTM/LA0011/2011 and PTDC/AAC-AMB/119172/2010. Catarina M. S. S. Neves also acknowledges FCT for the doctoral grant SFRH/BD/70641/2010.

Notes and references

1 N. V. Plechkova and K. R. Seddon, *Chem. Soc. Rev.*, 2008, **37**, 123–150.
2 P. Wasserscheid and T. Welton, *Ionic liquids in synthesis*, Wiley-VCH, Weinheim, 2008.
3 J. Ranke, S. Stolte, R. Stormann, J. Arning and B. Jastorff, *Chem. Rev.*, 2007, **107**, 2183–2206.
4 A. Kokorin, *Ionic Liquids: Theory, Properties, New Approaches*, ed. A. Kokorin, Rijeka, Croatia, 2011.
5 J. F. Brennecke and E. J. Maginn, *AICHE J.*, 2001, **47**, 2384–2389.
6 J. Huang, A. Riisager, R. W. Berg and R. Fehrmann, *J. Mol. Catal. A: Chem.*, 2008, **279**, 170–176.
7 R. L. Gardas and J. A. P. Coutinho, *Fluid Phase Equilib.*, 2008, **266**, 195–201.
8 J. F. Fernandez, J. Neumann and J. Thoeming, *Curr. Org. Chem.*, 2011, **15**, 1992–2014.
9 M. Petkovic, K. Seddon, L. Rebelo and C. Pereira, *Chem. Soc. Rev.*, 2011, **40**, 1383–1403.
10 D. B. Zhao, Y. C. Liao and Z. D. Zhang, *Clean: Soil, Air, Water*, 2007, **35**, 42–48.
11 J. S. Torrecilla, J. Palomar, J. Lemus and F. Rodriguez, *Green Chem.*, 2010, **12**, 123–134.
12 D. Coleman and N. Gathergood, *Chem. Soc. Rev.*, 2010, **39**, 600–637.
13 P. Stepnowski and A. Zaleska, *J. Photochem. Photobiol., A*, 2005, **170**, 45–50.
14 M. Czerwicka, S. Stolte, A. Muller, E. Siedlecka, M. Golebiowski and J. Kumirska, *J. Hazard. Mater.*, 2009, **171**, 478–483.
15 E. M. Siedlecka, M. Czerwicka, S. Stolte and P. Stepnowski, *Curr. Org. Chem.*, 2011, **15**, 1974–1991.
16 S. Stolte, J. Arning and J. Thoeming, *Chem. Ing. Tech.*, 2011, **83**, 1454–1467.
17 C. Abrusci, J. Palomar, J. Pablos, F. Rodriguez and F. Catalina, *Green Chem.*, 2011, **13**, 709–717.
18 J. Neumann, O. Grundmann, J. Thoeming, M. Schulte and S. Stolte, *Green Chem.*, 2010, **12**, 620–627.
19 G. W. Meindersma and A. B. de Haan, *Chem. Eng. Res. Des.*, 2008, **86**, 745–752.
20 P. Nockemann, K. Binnemans and K. Driesen, *Chem. Phys. Lett.*, 2005, **415**, 131–136.
21 J. Krockel and U. Kragl, *Chem. Eng. Technol.*, 2003, **26**, 1166–1168.
22 T. Schafer, C. M. Rodrigues, C. A. M. Afonso and J. G. Crespo, *Chem. Commun.*, 2001, 1622–1623.
23 C. M. S. S. Neves, M. G. Freire and J. A. P. Coutinho, *RSC Adv.*, 2012, **2**, 10882–10890.
24 J. L. Anthony, E. J. Maginn and J. F. Brennecke, *J. Phys. Chem. B*, 2001, **105**, 10942–10949.
25 M. Mahmoud and H. Al Bishri, *Chem. Eng. J.*, 2011, **166**, 157–167.
26 J. Palomar, J. Lemus, M. A. Gilarranz and J. J. Rodriguez, *Carbon*, 2009, **47**, 1846–1856.
27 J. Lemus, J. Palomar, F. Heras, M. A. Gilarranz and J. J. Rodriguez, *Sep. Purif. Technol.*, 2012, **97**, 11–19.
28 J. Lemus, J. Palomar, M. A. Gilarranz and J. J. Rodriguez, *Adsorption*, 2011, **17**, 561–571.
29 A. Farooq, L. Reinert, J. Levêque, N. Papaiconomou, N. Irfan and L. Duclaux, *Microporous Mesoporous Mater.*, 2012, **158**, 55–63.
30 J. Lemus, J. Palomar, M. A. Gilarranz and J. J. Rodriguez, *Ind. Eng. Chem. Res.*, 2013, **52**(8), 2969–2976.
31 L. Reinert, K. Batouche, J. Leveque, F. Muller, J. Beny, B. Kebabi and L. Duclaux, *Chem. Eng. J.*, 2012, **209**, 13–19.
32 X. Qi, L. Li, T. Tan, W. Chen and R. L. J. Smith, *Environ. Sci. Technol.*, 2013, **47**, 2792–2798.
33 R. Bansal and M. Goyal, *Activated carbon adsorption*, Taylor and Francis, Florida, 2005.
34 C. Y. Yin, M. K. Aroua and W. M. A. W. Daud, *Sep. Purif. Technol.*, 2007, **52**, 403–415.

35 C. M. S. S. Neves, A. R. Rodrigues, K. A. Kurnia, J. M. S. S. Esperança, M. G. Freire and J. A. P. Coutinho, *Fluid Phase Equilib.*, 2013, submitted.

36 M. J. Frisch, G. W. Trucks, H. B. Schlegel, G. E. Scuseria, M. A. Robb, J. R. Cheeseman, J. A. Montgomery Jr, T. Vreven, K. N. Kudin, J. C. Burant, J. M. Millam, S. S. Iyengar, J. Tomasi, V. Barone, B. Mennucci, M. Cossi, G. Scalmani, N. Rega, G. A. Petersson, H. Nakatsuji, M. Hada, M. Ehara, K. Toyota, R. Fukuda, J. Hasegawa, M. Ishida, T. Nakajima, Y. Honda, O. Kitao, H. Nakai, M. Klene, X. Li, J. E. Knox, H. P. Hratchian, J. B. Cross, V. Bakken, C. Adamo, J. Jaramillo, R. Gomperts, R. E. Stratmann, O. Yazyev, A. J. Austin, R. Cammi, C. Pomelli, J. W. Ochterski, P. Y. Ayala, K. Morokuma, G. A. Voth, P. Salvador, J. J. Dannenberg, V. G. Zakrzewski, S. Dapprich, A. D. Daniels, M. C. Strain, O. Farkas, D. K. Malick, A. D. Rabuck, K. Raghavachari, J. B. Foresman, J. V. Ortiz, Q. Cui, A. G. Baboul, S. Clifford, J. Cioslowski, B. B. Stefanov, G. Liu, A. Liashenko, P. Piskorz, I. Komaromi, R. L. Martin, D. J. Fox, T. Keith, M. A. Al-Laham, C. Y. Peng, A. Nanayakkara, M. Challacombe, P. M. W. Gill, B. Johnson, W. Chen, M. W. Wong, C. Gonzalez and J. A. Pople, *Gaussian03, revision B.05*, Wallingford, 2004.

37 J. P. Perdew, *Phys. Rev. B: Condens. Matter Mater. Phys.*, 1986, **33**, 8822–8824.

38 C. Sosa, J. Andzelm, B. C. Elkin, E. Wimmer, K. D. Dobbs and D. A. Dixon, *J. Phys. Chem.*, 1992, **96**, 6630–6636.

39 *COSMOtherm C2.1, release 01.06*, GmbH & Co. KG, Leverkusen, Germany, 2003.

40 J. Lemus, J. Palomar, M. Martin-Martinez, L. Gomez-Sainero, M. A. Gilarranz and J. J. Rodriguez, *Chem. Eng. J.*, 2012, **211–212**, 246–254.